Journal of Power Sources, 40 (1992) 137–146

Photocurrent spectroscopy and its application to the study of the lead/acid system

S. A. Campbell
Centre for Electrochemical and Materials Sciences, Department of Chemistry, University of St. Andrews, St. Andrews, Fife KY16 9ST, Scotland (UK)

L. M. Peter
Department of Chemistry, University of Southampton, Southampton SO9 5NH (UK)

J. S. Buchanan
Johnson Matthey Technology Centre, Blounts Court, Sunning Common, Reading RG4 9NH (UK)

Abstract

Photocurrent spectroscopy is a powerful, nondestructive, *in situ* technique which has been used to probe the semiconductor properties of anodic films on a variety of metals. In this paper the quantitative aspects of photocurrent spectroscopy are illustrated with examples taken from studies of lead in sulfuric acid.

Introduction

In recent years a wide range of *in situ* spectroscopic techniques has been applied to electrochemical systems to give information about components of the electrolyte or the electrode itself. Light absorption in solids can lead to the formation of excited states which are delocalized as free electron-hole pairs and are capable of generating a photocurrent or photovoltage. Systems can then be characterized by measuring the electrical response to the illumination. This is the principle of photocurrent spectroscopy. Semiconductor or insulator electrodes, in which significant bandgap limits electron-hole recombination, have attracted the most attention in this area although photoemission from metals has been studied [1].

The anodic oxidation of many metals produces semiconducting or insulating surface films which are often very thin, making any photoresponse very small. Conventional lock-in techniques allow such small photoeffects to be extracted from a large background and photocurrents of less than 10^{-12} A can be measured. In this paper the technique of photocurrent spectroscopy will be described and illustrated using examples from studies of anodic films produced on lead in sulfuric acid.

It has been known for some time that PbO forms underneath the $PbSO_4$ layer on lead when anodized in sulfuric acid [2–7]. This layer is important in determining, in part, the rate and extent of grid corrosion and hence the cycle life of the lead/acid battery. It has been suggested that additions of calcium and tin to the grid material influence the thickness of the grid layer [8] and that antimony may also have an effect. The detection and thickness measurement of very thin films (≤ 100 nm) in a multiphase anodic film is difficult using more traditional analysis techniques such as X-ray diffraction

0378-7753/92/$5.00

but are relatively staightforward using *in situ* photocurrent spectroscopy. This technique is capable of detecting films only a few nanometres thick on metals, gives information about the solid-state properties of the film enabling its identification, and can probe the oxide-substrate interface. Unlike Raman spectroscopy it uses very low-intensity light and does not perturb the system under study. Measurements of the flatband potential can indicate the local pH inside the film and, if the linear absorption coefficient is known, the film thickness can be accurately measured.

Photocurrent spectroscopy is a powerful and sensitive technique which may be applicable to the study of corrosion films in a wide range of systems and has been applied to the study of the lead/acid system [5].

The generation of a photocurrent in semiconductors

Figure 1 shows the fundamental difference in the electronic structures of metals and semiconductors. In a metal (Fig. 1(a)) an electron-hole pair, produced by the absorption of a photon, can relax rapidly (via path 1) so the quantum efficiency of photoemission (path 2) is small. The electron may also relax back in the solution (path 3) or be reinjected back into the metal (path 4). In semiconductors (Fig. 1(b)) geminate recombination is much slower, due to the forbidden energy gap, and the quantum efficiency of photoelectrochemical reactions with the conduction-band electron (path 1) or the valence-band hole (path 2) can approach unity.

Under depletion conditions the band structure of an n-type semiconductor at the electrode/electrolyte interface appears as in Fig. 2. Photogenerated electrons in the conduction band are expelled from the space charge region by the field and diffuse to the external circuit. Photogenerated holes in the valence band drift to the electrode surface where they may oxidize a solution species which will diffuse to the counter electrode to be reduced by the electron via the external circuit. This generates a photoelectrochemical current or 'photocurrent'.

This situation is simplified for a thin oxide film on a metal substrate as shown in Fig. 3. The space charge thickness (L_s) is large compared with the film thickness (L_f) and the field across the oxide is approximately linear. In Fig. 3 the oxide is n-type and under accumulation conditions (i.e., potential E less than the flatband potential E_{fb}) and the phenomenon of photoemission of electrons into the oxide from the substrate is illustrated. This mechanism can produce significant cathodic photocurrent.

The diffusion equation for the flux of minority carriers out of the space charge region for n-type depletion is:

$$D_p\left(\frac{\delta^2 p}{\delta x^2}\right)-\left(\frac{p(x)-p_0)}{\tau_p}\right)+g(x)=0 \qquad (1)$$

where D_p = hole diffusion coefficient, $p(x)$ = hole density at distance x from the interface, p_0 = equilibrium hole density, τ_p = hole lifetime and $= L_p/D_p$ where L_p = hole diffusion length, $g(x)$ = rate of hole photogeneration.

The solution of this equation is [9]:

$$I_{photo}=eI_0\left(1-\frac{\exp-(\alpha L_s)}{(1+\alpha L_p)}\right)+ep_0\frac{D_p}{L_p} \qquad (2)$$

where I_{photo} = photogenerated current, e = electronic charge, I_0 = incident light flux, α = monochromatic linear absorption coefficient, and L_s = thickness of the space charge region.

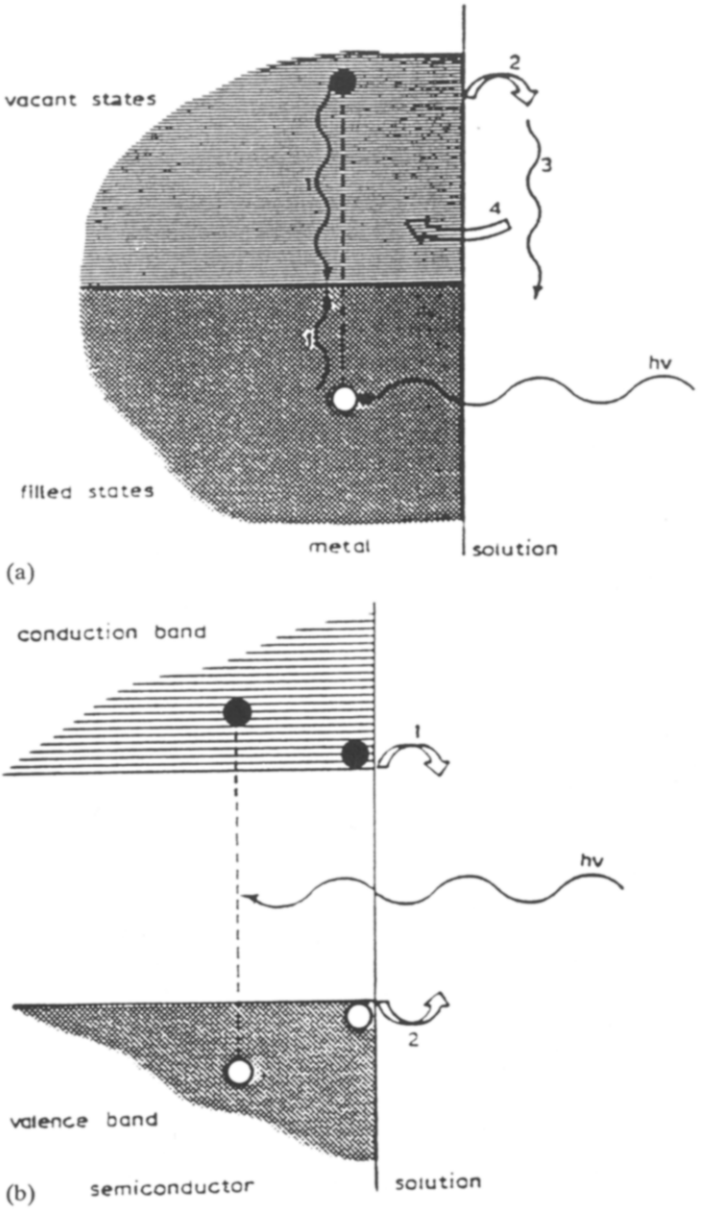

Fig. 1. (a) Optical excitation in a simple metal showing (1) rapid recombination, (2) photoemission, (3) relaxation in the solution and (4) back-injection of the electron from the solution; (b) optical excitation in an insulator or semiconductor where the forbidden energy gap prohibits recombination. In principle either conduction-band electrons (1) or valence-band holes (2) may react with solution species but minority carriers are most important for extrinsic semiconductors.

For a thin n-type film of thickness L_f where $L_f > L_s$ such as an anodic oxide on a metal, $p_0 \approx 0$, $L_s = L_f$ and $L_p = 0$ so eqn. (2) can be greatly simplified to:

$$I_{photo} = eI_0[1 - \exp - (\alpha L_f)] \quad (3)$$

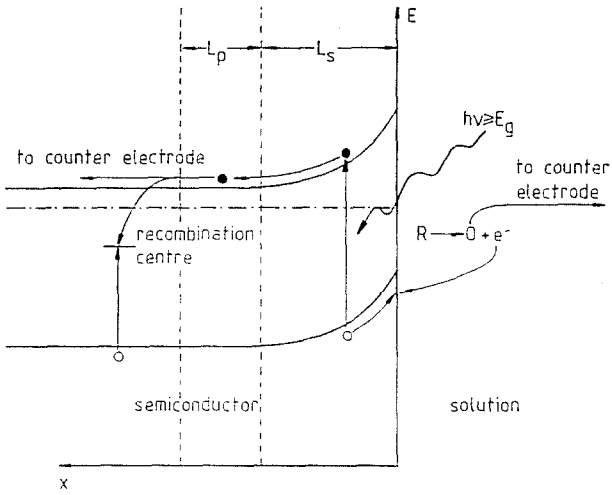

Fig. 2. Band diagram of a depleted n-type semiconductor in contact with a redox couple in solution, under illumination with light of energy greater than the bandgap energy E_g.

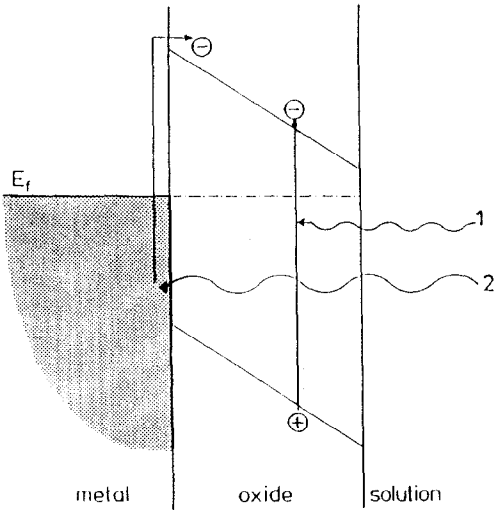

Fig. 3. Band diagram for a thin oxide film on a metal substrate in accumulation showing (1) photoexcitation of electrons across the oxide bandgap, and (2) photoemission of electrons from the metal into the conduction band of the oxide.

If L_f is small the exponential may be linearized, yielding:

$$I_{photo} = eI_0 \alpha L_f \tag{4}$$

Reflection of light from the metal substrate means that the light passes through the film twice; thus, assuming no losses in reflection at the oxide/metal boundary, the photocurrent conversion efficiency Φ is given by:

$$\Phi = I_{photo}/eI_0 = 2\alpha L_f \tag{5}$$

There is therefore a direct comparison between Φ and α. This enables the photoactive species to be identified and the thickness may be calculated.

Experimental

A schematic of the apparatus is shown in Fig. 4. Light from a 150 W xenon arc lamp passes through a single grating monochromator and is chopped mechanically at ≈ 27 Hz before being focussed onto the working electrode through a silica window in the electrochemical cell. The cell is otherwise a conventional three-compartment cell with a platinum gauze counter electrode and a commercial saturated calomel reference electrode (SCE). In this paper all potentials are quoted versus the calomel potential. A phase-sensitive detector (PSD) locked into the chopper frequency extracts the a.c. photoresponse from any faradaic background current, which may be several orders of magnitude larger.

There are two types of experiment. The wavelength which gives the maximum photoresponse is chosen and the photocurrent as a function of the potential is recorded simultaneously with a standard cyclic voltammogram. Then, holding the electrode at a potential which gives a steady photocurrent, the photocurrent as a function of wavelength is recorded. The monochromator is driven by a step motor controlled by the computer which acquires the data and corrects the spectrum, allowing for the characteristic lamp spectrum.

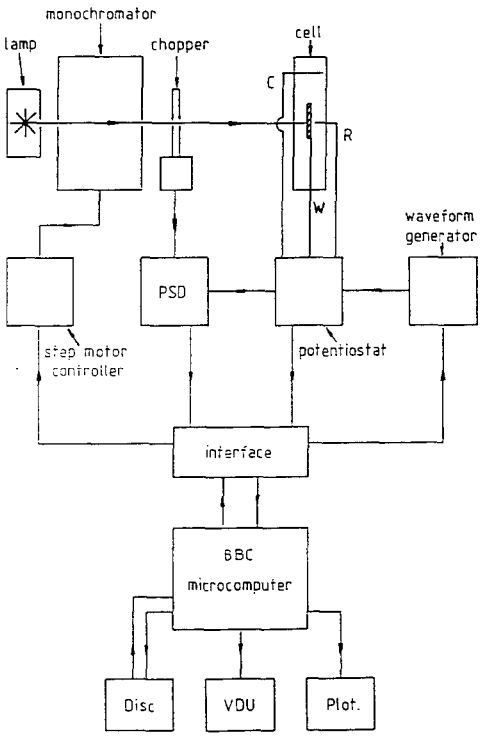

Fig. 4. Schematic diagram of the apparatus layout for photocurrent spectroscopy. PSD: phase-sensitive detector, VDU: visual display unit.

The photoresponse of anodic films on lead in sulfuric acid

Figure 5 shows the photocurrent recorded during cycling of a lead disc electrode in 0.5 M H_2SO_4 between -1.3 V and $+2.4$ V (i.e., between bare lead metal and anodic PbO_2) at 20 mV s^{-1}. It is interesting to note that, on the positive-going or forward sweep, the photocurrent is not detected until the potential reaches $+1.2$ V despite the formation of a $PbSO_4$ passive layer at ≈ -0.4 V. This is perhaps indicative of the time required to generate a complete PbO layer underneath the sulfate membrane. Positive of $+1.2$ V the photocurrent increases rapidly. The oxidation of the passive film to conducting PbO_2 causes the collapse of the photocurrent at $+2.3$ V. On sweep reversal the PbO_2 is reduced at $+1.2$ V and immediately the photocurrent returns, increasing to 200 nA before falling and passing through the current axis at -0.1 V and becoming cathodic. On reduction of the passive film to metallic lead the photocurrent collapses. The inversion of the photocurrent is of some importance. Polycrystalline tetragonal PbO is known to be n-type with a high minority carrier density [10] and therefore is not expected to give cathodic photocurrent when polarized negative of E_{fb} when it will be in accumulation. The appearance of a cathodic photocurrent is indicative of intrinsic or compensated behaviour. An explanation of this quasi-intrinsic behaviour of polycrystalline PbO has been proposed by Van den Broek [11] and later treated more fully by Albery and Bartlett [12]. The basis of their model is that as the crystallite size decreases the bulk properties of the crystals become dominated by surface states. Figure 6 shows how, as the crystallite size decreases, the surface-band bending raises the band edges and the Fermi level is pinned near the centre of the bandgap.

Holding the potential on the forward sweep at $+1.4$ V and on the reverse sweep at $+1.2$ V maintains a constant anodic photocurrent enabling the photocurrent spectrum, as a function of photon energy, to be recorded. The results are shown in Fig. 7 where they are compared with the absorption spectrum of tetragonal PbO [13]. The good

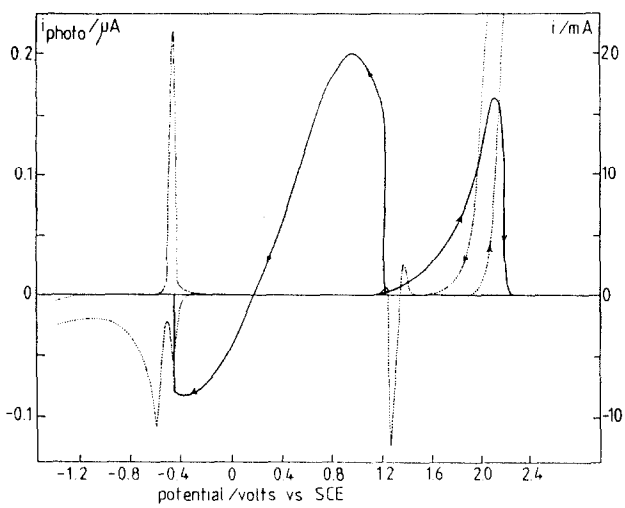

Fig. 5. Simultaneous measurement of the cyclic voltammogram (dotted line) and photocurrent (solid line) for a lead electrode (area 0.5 cm^2) in 0.5 M H_2SO_4 at ambient temperature; sweeprate 20 mV s^{-1}; illumination wavelength 340 nm; from ref. 5.

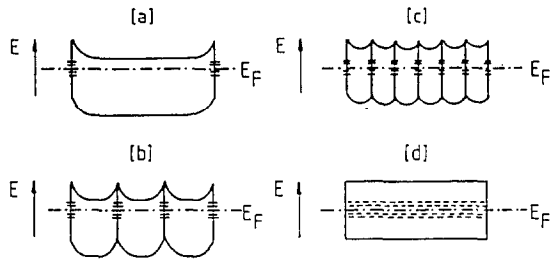

Fig. 6. Energy-band diagrams for n-type PbO in which the crystal dimensions are (a) much larger, (b) slightly larger, (c) slightly smaller and (d) much smaller than twice the surface barrier width measured in large crystals.

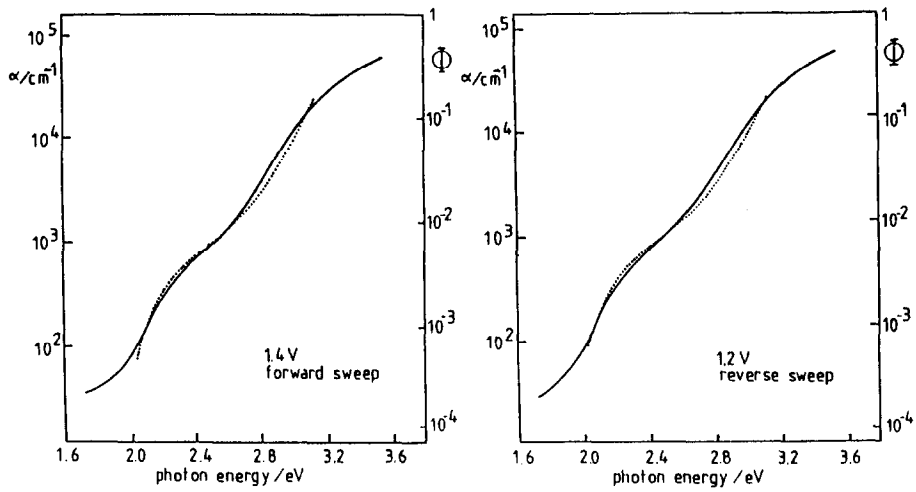

Fig. 7. Photocurrent spectra for lead in 5 M H_2SO_4 at the potentials shown compared with the absorption spectrum of tetragonal PbO (dotted line) [13]; from ref. 5.

fit of the spectra to that of the tetragonal PbO identifies the photoactive component of the anodic layer. Orthorhombic PbO has a larger bandgap (2.67 eV) and the absorption falls away much more quickly near the band edge [14]. By holding the potential at +0.1 V on the reverse sweep the cathodic photocurrent spectrum was obtained, as shown in Fig. 8 compared with the anodic photocurrent spectrum. The cathodic photocurrent spectrum shows an increased response at low photon energies. When PbO_2, electrodeposited on SnO_2-coated conducting glass, is reduced this additional photocurrent is absent [15], suggesting that it is due to photoemission from the lead substrate into the oxide. A Fowler plot of the photoemission efficiency (Fig. 9), constructed from data in Fig. 8, shows that the photoemission threshold occurs at 1.0 eV, which is very close to half the bandgap energy of tetragonal PbO. This supports the observation that the PbO is quasi-intrinsic as a result of its microcrystallinity. The band diagram for PbO on Pb at potentials negative of E_{fb} is as shown in Fig. 3.

Figure 10 shows the effect of temperature on the photocurrent spectrum recorded in 5 M H_2SO_4 after polarization of lead at +1.4 V for 50 min. The increase in photoresponse can be related to the PbO thickness via eqn. (5) and it can be shown

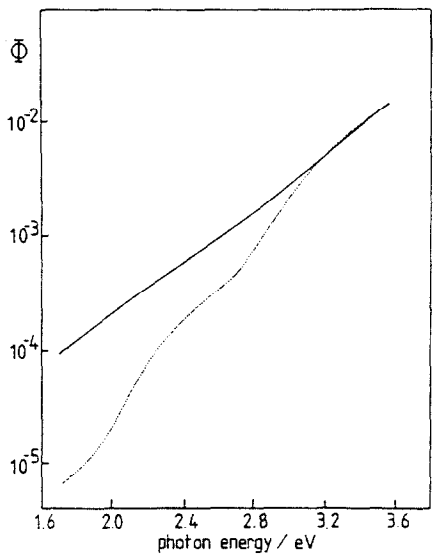

Fig. 8. Comparison of the cathodic photocurrent spectrum (measured at +0.1 V) with the scaled anodic spectrum (dotted line) for lead in 5 M H_2SO_4. The additional low-energy photoresponse is attributed to internal photoemission; from ref. 5.

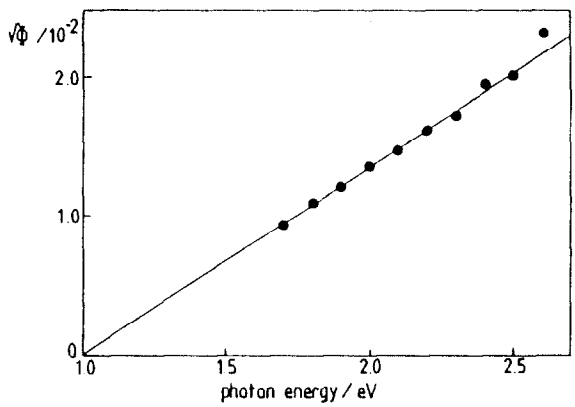

Fig. 9. Fowler plot of the photoemission efficiency constructed from the data in Fig. 8. The photoemission threshold occurs at half E_g for tetragonal PbO indicating quasi-intrinsic behaviour due to polycrystallinity (see Fig. 3).

that the PbO thickness varies linearly with temperature (Fig. 11). This is an important result, as it illustrates how photocurrent spectroscopy can be used to measure the thickness of the PbO underneath a relatively thick $PbSO_4$ layer on a lead substrate, a feat which is neither easy nor accurate by techniques such as X-ray diffraction. In the study of the lead/acid battery, corrosion and semiconductor electrochemistry photocurrent spectroscopy is a powerful tool for *in situ* studies which enable investigations to be carried out whilst maintaining electrochemical control.

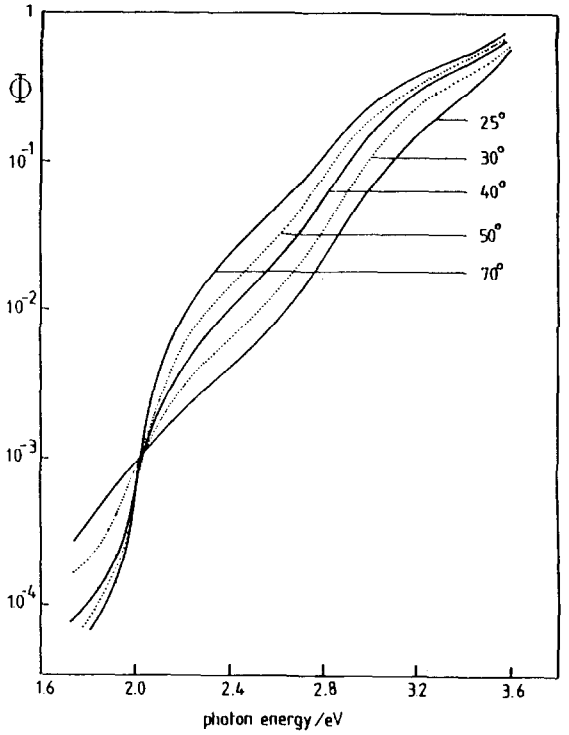

Fig. 10. The effect of temperature (°C) on the photocurrent spectrum from lead in 5 M H_2SO_4 after polarisation at +1.4 V for 50 min. The PbO is thicker at higher temperatures. Note also the effect on the spectrum near the band edge which suggests that the defect density varies with the temperature; from ref. 5.

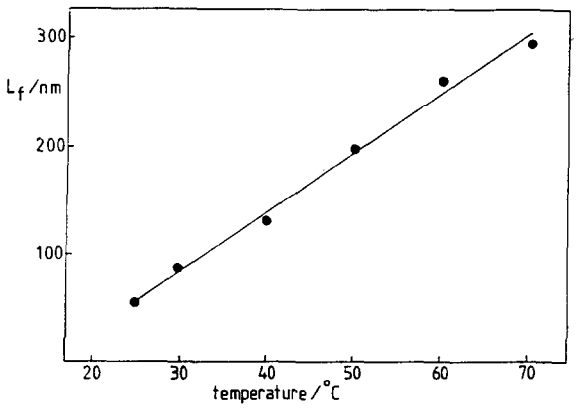

Fig. 11. Thickness of the PbO layer as a function of temperature, derived from data in Fig. 10.

References

1 R. G. Compton (ed.), *Comprehensive Chemical Kinetics, Vol. 29, New Techniques for the Study of Electrodes and their Reactions,* Elsevier, Amsterdam/New York, 1989, pp. 353–383.
2 D. Pavlov and N. Iordanov, *J. Electrochem. Soc., 117* (1970) 1103.
3 R. G. Barradas and D. S. Nadezhdin, *Can. J. Chem., 62* (1984) 596.
4 K. R. Bullock and M. A. Butler, *J. Electrochem. Soc., 133* (1986) 1085.
5 J. S. Buchanan and L. M. Peter, *Electrochim. Acta, 33* (1988) 127.
6 D. Pavlov, B. Monakhov, M. Maja and N. Penazzi, *J. Electrochem. Soc., 136* (1989) 27.
7 Y. Guo, *J. Electrochem. Soc., 138* (1991) 1222.
8 Y. Guo, *J. Electroanal. Chem.,* in press.
9 W. W. Gärtner, *Phys. Rev., 116* (1959) 84.
10 F. J. du Chatinier and J. Van den Broek, *Philips Res. Rep., 24* (1969) 392.
11 J. Van den Broek, *Philips Res. Rep., 24* (1969) 119.
12 W. J. Albery and P. N. Bartlett, *J. Electrochem. Soc.,* 131 (1984) 315.
13 J. Van den Broek, *Philips Res. Rep., 22* (1967) 367.
14 K. Iinuma, T. Seki and M. Wada, *Mater. Res. Bull., 2* (1967) 527.
15 S. A. Campbell and L. M. Peter, *J. Electroanal. Chem., 309* (1991) 213.